CSIRO PUBLISHING
www.publish.csiro.au/journals/fpb *Functional Plant Biology*, 2008, **35**, 885–899

Relative contributions of light interception and radiation use efficiency to the reduction of maize productivity under cold temperatures

Gaëtan Louarn[A,E], *Karine Chenu*[A,D], *Christian Fournier*[B,C], *Bruno Andrieu*[B,C] *and Catherine Giauffret*[A]

[A]INRA, UMR 1281 SADV, F-80203 Estrées-Mons, France.
[B]INRA, UMR 1091 EGC, F-78850 Thiverval-Grignon, France.
[C]AgroParisTech, UMR 1091 EGC, F-78850 Thiverval-Grignon, France.
[D]Present address: APSRU, Department of Primary Industries and Fisheries, PO Box 102, Toowoomba, Qld 4350, Australia.
[E]Corresponding author. Email: gaetan.louarn@mons.inra.fr

This paper originates from a presentation at the 5th International Workshop on Functional–Structural Plant Models, Napier, New Zealand, November 2007.

Abstract. Maize (*Zea mays* L.) is a chill-susceptible crop cultivated in northern latitude environments. The detrimental effects of cold on growth and photosynthetic activity have long been established. However, a general overview of how important these processes are with respect to the reduction of productivity reported in the field is still lacking. In this study, a model-assisted approach was used to dissect variations in productivity under suboptimal temperatures and quantify the relative contributions of light interception (PAR_c) and radiation use efficiency (RUE) from emergence to flowering. A combination of architectural and light transfer models was used to calculate light interception in three field experiments with two cold-tolerant lines and at two sowing dates. Model assessment confirmed that the approach was suitable to infer light interception. Biomass production was strongly affected by early sowings. RUE was identified as the main cause of biomass reduction during cold events. Furthermore, PAR_c explained most of the variability observed at flowering, its relative contributions being more or less important according to the climate experienced. Cold temperatures resulted in lower PAR_c, mainly because final leaf length and width were significantly reduced for all leaves emerging after the first cold occurrence. These results confirm that virtual plants can be useful as fine phenotyping tools. A scheme of action of cold on leaf expansion, light interception and radiation use efficiency is discussed with a view towards helping breeders define relevant selection criteria.

Additional keywords: architecture, chilling stress, elite inbreds, light transfer model, structural model, *Zea mays*.

Introduction

Plant response to temperature is one of the most important factors governing the yield of crops. Many species are, however, cultivated well outside their original zones of natural selection and, hence, experience temperatures out of their optimal range. Agronomists usually distinguish three categories with respect to the damages induced by low temperatures: chill-susceptible plants are affected by temperatures below 10–15°C; chill-tolerant but freezing susceptible plants are unable to survive freezing; and lastly, freeze-tolerant plants are able to acclimatise to and survive temperatures well below freezing (Pearce 1999).

Maize is a typical chill-susceptible species of subtropical origin which has become a major crop in temperate areas. Negative impacts of temperatures below 15°C on growth (Blondon *et al*. 1980; Miedema 1982; Pollock and Eagles 1988; Verheul *et al*. 1996) and photosynthetic activity (Blondon *et al*. 1980; Long 1983; Long *et al*. 1983; Dolstra *et al*. 1994; Verheul *et al*. 1995) have been identified. Generally, decreased leaf expansion rates under chilling conditions are associated with a lower rate of cell production in the meristematic zone but not with smaller cells (Ben Haj Salah and Tardieu 1995; Rymen *et al*. 2007). At the same time, reduced rates of carbon assimilation are usually related to reductions of stomatal aperture (Massacci *et al*. 1995), modifications in chloroplast ultrastructure (Nie *et al*. 1995; Sowiński *et al*. 2005), changes in pigment composition (Haldimann 1998), decreased quantum efficiency (Fryer *et al*. 1995; Verheul *et al*. 1995) and limitations of the flow of assimilates between mesophyll and bundle sheath cells (Sowiński *et al*. 2003). Despite this detailed knowledge at microscopic and molecular levels, a general overview of how these processes interact and of how important they are with respect to the reduction of productivity is still lacking, but is needed to properly analyse the detrimental effects reported in the field (Greaves 1996). This is becoming a critical issue in a context of sustainable agriculture because, in the northern

10.1071/FP08061 1445-4408/08/100885

fringe of the area of cultivation, earlier sowing would allow a better fit between crop cycle and overall resource availability (Pollock and Eagles 1988; Lauer *et al.* 1999). Early-sown cold-tolerant plants are expected to maximise early season radiation interception while avoiding the concomitance of the first water shortages with flowering stage. Breeders are, thus, seeking original adaptation strategies enabling maize to grow more efficiently under cool temperatures (Greaves 1996).

To address the question of which factor limits productivity, a classical approach relies on the linear relationship between biomass production (dry weight, DW) and intercepted radiation (cumulated photosynthetically active radiation intercepted, PAR_c), which is consistently observed in conditions where neither water nor mineral nutrients are limiting (Heath and Hebblethwaite 1987; Lecoeur and Ney 2003). Radiation-use efficiency (RUE) is defined as the slope of the relationship over a given period of time (Sinclair and Muchow 1999).

$$DW = RUE \times PAR_c \qquad (1)$$

Since such linear relationship does occur for a wide range of crops when observed at canopy level for time periods between 1 week and a few months (Monteith 1977), it is possible to link departures from the linearity to the occurrence of some specific constraint (e.g. low nitrogen availability, Sinclair and Horie 1989). Such a framework is a great asset for analysing maize productivity fluctuations under cold conditions: it enables discrimination between light-interception-related (through PAR_c) and photosynthesis-related (through RUE) variations in crop productivity. In the present study, we applied it to maize stands grown in a realistic range of climatic scenarios.

A particular challenge in conducting such a study was to take into consideration the heterogeneous nature of a maize (*Zea mays* L.) canopy during and following cold events. Indeed, chilling temperatures most likely occur in April and May, when plants are seedlings composed of a couple of leaves. At this stage, estimating stand light capture and PAR_c accurately using direct measurement methods is practically impossible (Gallo and Daughtry 1986; Sinclair and Muchow 1999). Furthermore, a side-effect of cold occurring between sowing and emergence is to increase canopy heterogeneity by decreasing the percentage of germination and by spreading out the variability in emergence dates (Eagles and Hardacre 1979; Miedema 1982). These erratic emergences result in randomly missing plants and a larger plant to plant variability later in the cycle. A suitable way to overcome this difficulty could be the use of individual-based simulation models able to account for the dynamic evolution of plant architecture in the field (Fournier and Andrieu 1998). Their coupling with light transfer models theoretically makes it possible to quantify light interception at the stand level taking into account the actual emergence pattern and the architecture of the plants.

The objectives of this study were: (1) to assess the feasibility and reliability of such a modelling approach to estimate light interception for maize seedlings as well as for mature plants of different genotypes, and (2) to apply it to dissecting variations in dry matter production under suboptimal temperatures and identifying the relative contributions of RUE and of the architectural traits involved in light interception. To do so, we conducted three field experiments with two cold-tolerant inbred lines and two sowing dates. The 3-D model ADEL-maize (Fournier and Andrieu 1998) was calibrated and evaluated for each situation. It was used, together with a radiosity model (Chelle and Andrieu 1998), to calculate light interception by plants. The processes involved in the plant response were finally analysed in order to help breeders identify key performance traits to improve elite inbred pools with respect to cold tolerance.

Materials and methods

Experimental design

Field experiments were conducted at Estrées-Mons (49°N, 3°E, 85 m), France, in 2005, 2006 and 2007, with the cold-tolerant maize (*Zea mays* L.) inbred lines F2 and F286, which are early flint lines of temperate origin differing in their architectural characteristics. Each year, both lines were grown at two sowing dates referred to as ‘early’ for first week of April and ‘normal’ for first week of May. For each sowing date, the experimental plots, each containing a single genotype planted at 0.12×0.8 m plant spacing on eight rows of 40 plants, were randomly positioned in a split-plot design, with three replications in the form of north–south-orientated blocks. In 2005 and 2006, 20 mm irrigation was applied once a week from 15 June. In 2007, due to an exceptionally rainy summer, no irrigation was supplied.

The six year × sowing date combinations (referred to as ‘treatments’) resulted in contrasting temperature regimes presented in Fig. 1. Each year the early sown plants experienced severe periods of cold stress. These periods occurred at different stages of seedling establishment every year, significant cold waves being registered around ligulation of the first leaf, of the second and of the third leaves for 2005, 2006 and 2007, respectively. In the normal sowing of 2006, daily average temperatures remained above 15°C, which is the threshold for cold stress in maize (Miedema 1982), throughout the cycle. However, normal sowings in 2005 and 2007 encountered cold events later in their development, at stages nine and five liguled leaves, respectively. Treatments also strongly differed in incoming PAR radiation (Table 1). Light availability was lower in 2007, as compared with 2005 and 2006. In 2005 and 2007, crops experienced similar light levels during seedling establishment (from emergence to seven liguled leaves) and during later growing stages until flowering (seven liguled leaves to tasseling). Conversely, early and late 2006 sowings experienced reversed patterns of light availability, the early sowing having the most favourable sequence for biomass production (high light levels concomitant with higher development stages). Altogether, these six climate conditions generated a range of temperature and light enabling us to test maize response to cold events.

Meteorological data

Air temperature and relative humidity were measured on the experimental site with a capacitive hygrometer (50Y, Campbell Scientific Ltd, Shepshed, Instruments Ltd, Powys, UK) placed in a standard, naturally aspirated radiation shield, at a height of 2.5 m above the soil. Incoming global radiation was

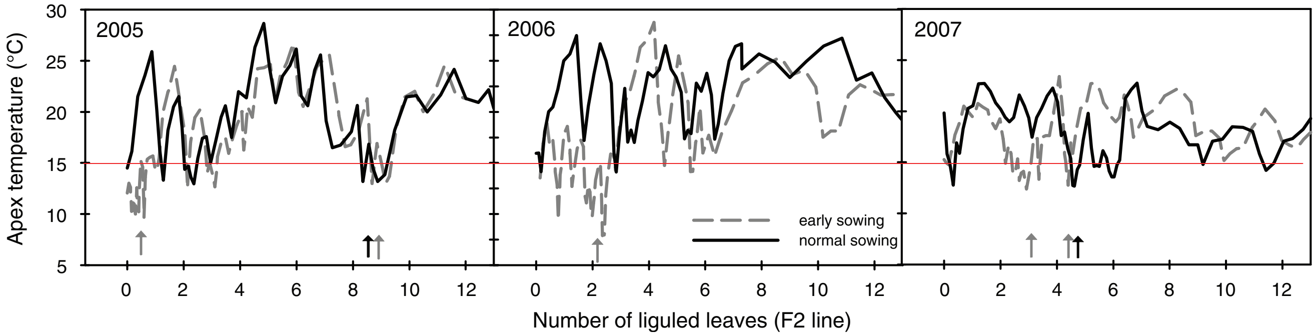

Fig. 1. Apex temperature *v.* plant development expressed in number of liguled leaves for the early and normal sowings of the F2 inbred line during the years 2005, 2006 and 2007. The horizontal line represents the temperature below which chilling injury is expected to occur in maize. Arrows show peaks of major cold events for early (grey) and normal (black) sowings.

Table 1. Average daily incoming PAR energy (MJ m^{-2}) for the three years of experiment (2005, 2006, 2007) on the F2 line

For each sowing date (early, normal) the average is calculated for three periods of time: emergence to seven liguled leaves, seven liguled leaves to flowering and emergence to flowering

Period	2005		2006		2007	
(no. of liguled leaves)	Early	Normal	Early	Normal	Early	Normal
0–7	10.5	11.0	8.9	11.3	8.6	8.2
7–flowering	9.4	9.6	11.6	9.9	8.2	9.8
0–flowering	10.2	10.5	9.4	11.0	8.5	8.7

measured with a pyranometer (LP02, Campbell Scientific Ltd, Shepshed, Instruments Ltd, Powys, UK) and photosynthetically active radiation (PAR) was measured with a PPFD sensor (LI-190SB: Li-Cor, Lincoln, NE, USA). Apex temperature was estimated using soil temperature before tassel initiation (measured by thermistors placed 3-cm deep) and sheath temperature after tassel initiation (monitored with thermocouples copper-constantan placed in the sheath of the last liguled leaf). Data were stored in a datalogger (CR10X, Campbell Scientific Ltd, Shepshed, Leicestershire, UK), with measurements taken every 30 s and averaged over 900 s).

An equivalent thermal time was calculated from apex temperature measurements using the equation of Yan and Hunt (1999), adjusted to a base temperature of 9.8°C in the linear part of the response.

Plant measurements

For each plot, five plants were chosen so that their development was close to the median for that treatment and were tagged at the stage of one liguled leaf. Two to three times a week, the number of visible, liguled and senescent leaves was counted. These records enabled us to define the dates of sampling for the destructive measurements described below.

Aboveground biomass was measured by harvesting five median plants per plot, selected on the basis of their stage of development and of the length of the higher liguled leaf. In 2006 and 2007, harvests took place at stages of one, three, four, five, six, seven and eight liguled leaves and at silking; in 2005 harvests took place at stages of three, seven and ten liguled leaves and at silking. Harvested plants were dried in an oven (70°C, 48 h) and weighed individually.

Plant architecture was characterised at stages of five and eight liguled leaves and at silking on five median plants per plot. This included measurements of the dimensions of mature organs (lamina length and width, sheath length, internode length, basal and apical stem diameters), and measurement of the curvature of leaf midribs and the 2-D leaf shape (Prévot *et al.* 1991). Prévot's curvature model assumes that the midrib belongs to a vertical plane, and its curvature can be described by a parabolic curve for the ascending part and by a portion of ellipse for the descending part, when it exists. Model parameters were estimated using the silhouette method for data acquisition (acquisition of gramineous leaf geometry by taking pictures of whole plant profiles, Bonhomme and Varlet-Grancher 1978), image analysis for midrib points extraction (ImageJ software, http://rsb.info.nih.gov/ij/, accessed 19 September 2008), and optimisation for parameter identification (*lm* procedure, R software, http://www.r-project.org/, accessed 19 September 2008). Similarly, 2-D leaf shapes, i.e. the shapes of fully expanded laminae developed on a plane surface, were characterised for both genotypes according to the second order polynomial model proposed in Prévot *et al.* (1991) that links normalised lamina width to the normalised distance to the ligule. Average leaf elevations were finally derived from (i) elevation angles between consecutive midrib points extracted from the silhouette pictures, and (ii) leaf shape measurements, by weighting leaf elevation at regularly spaced curvilinear abscissa with normalised lamina width at this position.

We measured two canopy structure indices. Ground cover, the fraction of soil covered with canopy elements, was estimated once a week. Digital photograph were taken at a height of 2.5 m right above the 4th row of each plot. Ground cover was then determined using the Optimas software (Optimas 6.5, BioScan, Edmond, WA, USA) to isolate maize canopy from soil on the images. We also monitored the ratio between the light transmitted to the soil and incoming light. To do so, each experimental plot was equipped at least one day every 2 weeks with a linear PAR sensor at the ground level (Solems SA, Palaiseau, France), except for the F286 inbred line in 2007 for which low germination rates made it impossible to determine relevant sensor positions. In all other cases measurements were performed on a 1-row-wide transect on both sides of the 4th row.

Estimation of intercepted PAR

According to the analytical framework described in Eqn 1, cumulative intercepted PAR determines potential crop productivity. This key variable is difficult to measure accurately in heterogeneous canopy structures (such as those composed of seedlings), thus we developed an approach coupling 3-D stand modelling and radiative transfer simulation to infer its value.

Architectural model description

We used the model ADEL-maize described in Fournier and Andrieu (1998) and based on the L-system modelling principles (see Prusinkiewicz and Lindenmayer 1990; Prusinkiewicz *et al.* 1997; for a general overview) to simulate 3-D plant structures. Only the main features of the model and the specific adaptations made in this study are presented here. The model was implemented using the Graphtal software facilities (Streit 1992).

L-systems generally represent plants as strings of modules (a module being any structural unit repeated in the global structure – here, apices, leaves and internodes) and feature growth and development through a set of production rules enabling iterated rewriting of this string. In ADEL-maize, the initial module is an apex and two sets of production rules are defined, determining physiological processes (organogenesis and subsequent organ elongation) and geometrical features (organ triangulation according to geometric primitives), respectively.

The production rules associated with the apex describe successive initiation of phytomers, consisting of two other modules: an internode and a leaf primordium. No axillary bud is considered. The production of phytomers stops when the apical meristem enters its reproductive stage (determined empirically) and initiates the tassel. Subsequent steps of development are derived from observation of quasi-sequential events in the region of cell division of grass leaves (Meiri *et al.* 1992; Ben Haj Salah and Tardieu 1995). For each phytomer, an individual leaf blade elongates first, followed by leaf sheath at the end of blade growth, and by internode at the end of sheath growth. Leaf lamina elongation is assumed to follow a broken line function characterised with three parameters: (i) the delay between thermal time of phytomer initiation (TTn) and beginning of elongation (DIE), (ii) the growth rate (GR), and (iii) the delay between phytomer initiation and ligulation (DIL) fixing the end of lamina extension. We defined a supplemental parameter to account for leaf senescence (SPAN, leaf live span, deduced from measurements of leaf ligulation and senescence) and introduced a new production rule making the leaf fall at the end of this period.

In order to accurately reproduce the growth dynamics observed in the field, and to facilitate integration of the impact of cold on growth and organogenesis, the coordination of development between the successive phytomers, the individual leaf elongation rates and the final organ dimensions were forced to match field measurements. In this constrained version of the model, parameters TTn and DIE were derived from the measurements of leaf emergence. The first five primordia were supposed to be present in the seed (at TTn = 0). For the initiation of the following phytomers, the plastochron (thermal time elapsing between the initiation of consecutive primordia) was assumed to equal two measured phyllochrons (thermal time elapsing between the emergence of two consecutive leaf tips). These assumptions are empirically supported by a preliminary greenhouse experiment involving the two studied inbred lines (five primordia in the seed for both lines), as well as by results obtained on other genotypes (Padilla and Otegui 2005; Andrieu *et al.* 2006; Chenu *et al.* 2008*a*). DIE was set to be 80% of the time elapsing between leaf initiation and leaf emergence on the basis of recent results on the ontogeny of maize leaves (Déa cultivar, Andrieu *et al.* 2006; Chenu *et al.* 2008*a*). Lastly, for leaves, DIL parameters were directly derived from measurements of ligulation, and individual leaf extension rates were computed as the ratio between final lamina length and the duration of leaf elongation (DIL – DIE). A similar approach was taken to simulate the elongation of internodes from their final organ length, assuming a constant elongation rate. The duration of internode elongation was assumed to be 60% of that of leaf on the same phytomer, based on, unpubl. data for the Déa cultivar.

The rules used to generate the geometric representation of maize were mostly as described by Fournier and Andrieu (1998). A parameterisation of the increase in basal diameter with respect to cumulated thermal time since emergence was introduced, parameters being fitted for each genotype according to stem diameter measurements. The representation of leaves followed the parameterisation presented above (Prévot *et al.* 1991). The limited number of samples collected in each treatment (~10 leaves at each rank along the stem) did not allow investigating co-variations of the Prévot's parameters with the phytomer rank and the growing conditions experienced. In order to represent only realistic leaves, we avoided random generation of original set of parameters, and instead, opted for a strategy of random drawing of whole leaf sets into the database of measured leaves. Random samplings of whole leaf sets were performed according to genotype, to phytomer rank and treatment. When simulating emerging leaves, the angle of insertion of the lamina was considered to change linearly with thermal time from the vertical (at leaf emergence) to its measured value (at the end of leaf elongation).

Computation of light interception at the canopy level

The 3-D structural model described above was used to simulate virtual plots of 4 rows × 14 median plants (5.4 m^2, Fig. 2). The positions of plants missing in the field were recorded and taken into account in these simulations. Each treatment was simulated for 10 growth stages regularly spaced between emergence and silking. The time course of any variable was calculated by interpolating between these dates.

Each 3-D stand generated was used as an input to the radiative transfer model CANESTRA (Chelle and Andrieu 1998). Radiative budgets of individual plant elements and of the soil compartment were calculated, considering direct incoming light only. Optical properties of leaves were assumed to be identical for both genotypes and all treatments. They were derived from measurements on the Déa cultivar (reflectance and transmittance equal to 0.09 and 0.04, respectively). Light simulations were

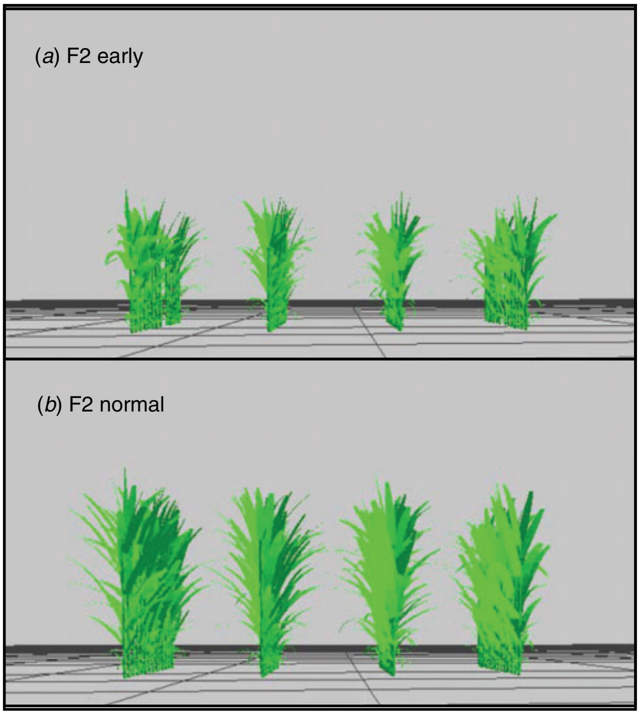

Fig. 2. Examples of simulated 3-D stands at 600°Cd in 2005 (F2 inbred line).

performed for overcast sky and for direct sunlight. Overcast conditions were approximated using 162 light sources positioned in the centres of nine elevations × 18 azimuths sectors, light intensities being computed according to the universal overcast model (Hutchinson *et al.* 1980). Direct sunlight was determined using astronomical formulae for sun position (one position per hour, Jones 1992) and estimated direct light intensity (see below). This approach allowed calculation of the light interception efficiency (ratio between intercepted and incoming PAR radiation at the stand level) separately for direct and diffuse light sources ($\varepsilon_{i,\mathrm{direct}}$, $\varepsilon_{i,\mathrm{diffuse}}$). The radiative transfer simulations thereby defined two boundary curves of ε_i, per treatment. Once these two components were estimated, the actual daily light interception efficiency (ε_i) was calculated as:

$$\varepsilon_i = (1-f)\times\varepsilon_{i,\mathrm{direct}} + f\times\varepsilon_{i,\mathrm{diffuse}}, \qquad (2)$$

where *f* is the fraction of diffuse radiation in the global incoming light. Daily *f* values were calculated from global incoming light measurements using the empirical model of Spitters *et al.* (1986). Daily values of intercepted PAR ($\mathrm{PAR}_{\mathrm{inc,d}}$, MJ) were obtained by multiplying $\varepsilon_{i,\mathrm{d}}$ by the daily amount of incoming PAR energy. Finally, cumulated intercepted PAR ($\mathrm{PAR}_{\mathrm{c,t}}$) was calculated as:

$$\mathrm{PAR}_{\mathrm{c,t}} = \sum_{d=\mathrm{emergence}}^{d=t} (\varepsilon_{i,\mathrm{d}}\times\mathrm{PAR}_{\mathrm{inc,d}}). \qquad (3)$$

Assessment of simulation outputs

In order to check the reliability of the calculation of intercepted light, we assessed the model outputs at two levels. First, we compared 3-D simulations to real canopies using the ground cover. For each plot, virtual scenes were generated at the thermal time where field pictures were taken. Computer images were then generated using the POV-Ray ray tracing software (Persistence Of Vision Ray Tracer, version 3.5, http://www.povray.org, accessed 19 September 2008) mimicking the actual camera characteristics (pinhole type, with actual focal length, camera position and camera height). These images were processed in the same way as the photographs taken in the field. Second, we compared simulated ε_i with the measured ratios between the light transmitted to the soil and incoming light.

Estimation of RUE

A large number of approaches have been used for estimating RUE, as discussed by Sinclair and Muchow (1999). Here, RUE was estimated for 'PAR intercepted radiation' according to the terminology proposed by Bonhomme (2000) and taking into account only the aboveground biomass. For each experimental plot, RUE was estimated as the slope of the linear regression between simulated PAR_c and measured crop biomass (which equals the average aboveground biomasses of the median plants multiplied by the actual planting density).

Long-term RUE was determined for two periods: emergence to seven liguled leaves, and emergence to silking. This allowed comparison of treatments for their behaviour during the period of seedling establishment and throughout the whole experiment, respectively. We also estimated RUE on short time intervals, between consecutive harvests (approximately a week). The calculation of 'short-term' RUE aimed at capturing the transient effects of cold temperatures on the conversion of intercepted energy into biomass (Rochette *et al.* 1996).

Relative contributions of PAR_c and RUE to biomass variations

It follows from Eqn 1 that the ratio between biomasses of early and normal sowings can be written:

$$\frac{\mathrm{DW}_{\mathrm{early}}}{\mathrm{DW}_{\mathrm{normal}}} = \frac{\mathrm{RUE}_{\mathrm{early}}}{\mathrm{RUE}_{\mathrm{normal}}}\times\frac{\mathrm{PAR}_{\mathrm{c,early}}}{\mathrm{PAR}_{\mathrm{c,normal}}}. \qquad (4)$$

When $\mathrm{DW}_{\mathrm{early}}$ is different to $\mathrm{DW}_{\mathrm{normal}}$, i.e. when the early sowing has an effect on the biomass production, Eqn 4 can be written as:

$$1 = \frac{\log(\mathrm{RUE}_{\mathrm{early}}/\mathrm{RUE}_{\mathrm{normal}})}{\log(\mathrm{DW}_{\mathrm{early}}/\mathrm{DW}_{\mathrm{normal}})} + \frac{\log(\mathrm{PAR}_{\mathrm{early}}/\mathrm{PAR}_{\mathrm{c,normal}})}{\log(\mathrm{DW}_{\mathrm{early}}/\mathrm{DW}_{\mathrm{normal}})}. \qquad (5)$$

Two parameters, corresponding to the two terms in the right side of this equation, namely $k = \log(\mathrm{RUE}_{\mathrm{early}}/\mathrm{RUE}_{\mathrm{normal}})/\log(\mathrm{DW}_{\mathrm{early}}/\mathrm{DW}_{\mathrm{normal}})$ and $1-k$, can be defined, so as Eqn 4 becomes:

$$\frac{\mathrm{RUE}_{\mathrm{early}}}{\mathrm{RUE}_{\mathrm{normal}}}\times\frac{\mathrm{PAR}_{\mathrm{c,early}}}{\mathrm{PAR}_{\mathrm{c,normal}}} = \left(\frac{\mathrm{DW}_{\mathrm{early}}}{\mathrm{DW}_{\mathrm{normal}}}\right)^{k}\times\left(\frac{\mathrm{DW}_{\mathrm{early}}}{\mathrm{DW}_{\mathrm{normal}}}\right)^{1-k}. \qquad (6)$$

Parameters k and $(1-k)$ were taken as indicators of the contribution of RUE (k) and PAR_c $(1-k)$, respectively, in the variation of dry weight accumulation. k and $(1-k)$ can take any real value. They have particular meaning at $k = 1$ (the difference in

RUE explains completely the dry matter variation, as $DW_{early}/DW_{normal}=RUE_{early}/RUE_{normal}$), $k=0.5$ (both RUE and PAR_c contribute equally to DW variations) or $k=0$ (the difference in PAR_c explains completely the variation, $DM_{early}/DM_{normal}=PAR_{c,early}/PAR_{c,normal}$). If $k>1$ (and, thus, $1-k<0$), then PAR_c overcompensates for a positive RUE effect on dry weight. If $k<0$ (and, thus, $1-k>1$), then RUE overcompensates for a positive PAR_c effect on dry weight.

When DW_{early} equals DW_{normal}, i.e. when the early sowing has no effect on the biomass production, k and $(1-k)$ cannot be computed (as there is no biomass variation to explain). If RUE and PAR_c do vary in the same time, they perfectly compensate for each other and the magnitude of their variation can be evaluated directly by the ratios presented in Eqn 4.

Sensitivity analysis

Architectural traits potentially affecting ε_i were ranked by carrying out a sensitivity analysis quantifying their impact on PAR_c under constant environmental conditions ($t=22.4$°C, PAR = 10.43 MJ day^{-1}, equivalent to the average condition for the normal sowing of 2005). Eight cases combining the extreme leaf area profiles, leaf angles and rates of leaf emergence encountered were studied (Table 2). Virtual plots of four rows × 14 median plants (5.4 m^2) were simulated at eight regularly spaced growth stages between emergence and silking. Radiative transfer and PAR_c computation were performed as mentioned above, except that only the diffuse sky condition was considered in order to avoid any restriction of the result's validity due to a particular sun track/sowing date.

Statistical analysis

The ANOVA/MANOVA procedure of Statistica 6.0 (Statsoft, Tulsa, OK, USA) was used to test for significant differences between means. The *t*-test for independent samples was chosen when only two populations had to be compared. Analysis of covariance (ANCOVA) was used to compare slopes and intercepts of linear relationships.

Table 2. Characteristics of the plant growth scenarios used for the sensitivity analysis

Symbols + and – refer to extreme value observed in normal and early sowings, respectively, and correspond to treatments F2-normal-2005 and F2-early-2005 for leaf area profiles, F2-early-2007 and F2-early-2005 for phyllochrons, F286-early-2007 and F2-early-2005 for leaf angles, respectively

Scenario no.	Leaf area profile	Phyllochron	Leaf angles	Corresponding treatment
1	–	–	–	F2-early 2005
2	+	–	–	None
3	–	+	–	None
4	+	+	–	None
5	–	–	+	None
6	+	–	+	None
7	–	+	+	None
8	+	+	+	None

Simulated and measured values were compared using the root mean square error (RMSE) and bias (B) of the model, calculated as follows:

$$\mathrm{RMSE}=\sqrt{\frac{\sum_{i=1}^{n}(s_i-m_i)^2}{n}}, \tag{7}$$

$$\mathrm{B}=\frac{\sum_{i=1}^{n}(s_i-m_i)}{n}, \tag{8}$$

where s_i and m_i are the ith simulated and measured values, respectively, and n is the number of observations.

Results

Assessment of the methodology

The first step in evaluating the modelling approach consisted of a comparison between real and simulated canopy structures using ground cover (Fig. 3). For the two inbred lines, simulated values of ground cover were consistent with field data in terms of both absolute values (RMSE <2.9%; |B| <0.7%) and in the reproduction of the inter-row variability (pairwise *t*-test on the standard deviations, $P>0.39$). Simulation accuracy was proportionally better for mature canopies (CV = 7% for plants having more than seven liguled leaves) than for early stages of development (CV = 23%), although there were limited consequences in terms of absolute estimation of the ground cover (RMSE <1.0%, |B| <0.1% before seven liguled leaves).

We further assessed model outputs on the basis of light interception properties. Figure 4 shows how ε_i changed with thermal time in the different treatments. The 3-year follow-up covered a wide range of canopy structures as shown by the contrasting dynamics of observed ε_i. Maximum values reached and differences between early and normal sowings varied among years, indicating differential effects of the treatments on canopy architecture. Early sown stands systematically displayed lower ε_i values at flowering (~700°Cd) than their respective normally sown plants. The difference was significantly larger in 2005 as compared with the 2 other years. The modelling approach simulated quite accurately the variability between years in ε_i values at flowering (RMSE <7%; |B| <5%; CV <16%). Hence, we assumed from this point on that it was possible to use the models to quantify light interception by maize stands of the two studied lines in the range of climatic sequences experienced.

Origin of the variations of maize productivity under cold temperatures

Productivity in terms of above ground biomass before flowering, light interception and long-term RUE are presented in Fig. 5. Dry matter production varied significantly among treatments. At flowering maximum values were reached for the two genotypes for normal sowings of 2005 (Fig. 5*b*). In all treatments, biomass production was higher for F286 than for F2. They were significantly lower for early sowings than for normal ones, except for F2 in 2006 (no significant reduction). The difference in productivity at flowering between early and normal sowings varied between years, being maximal in 2005 and

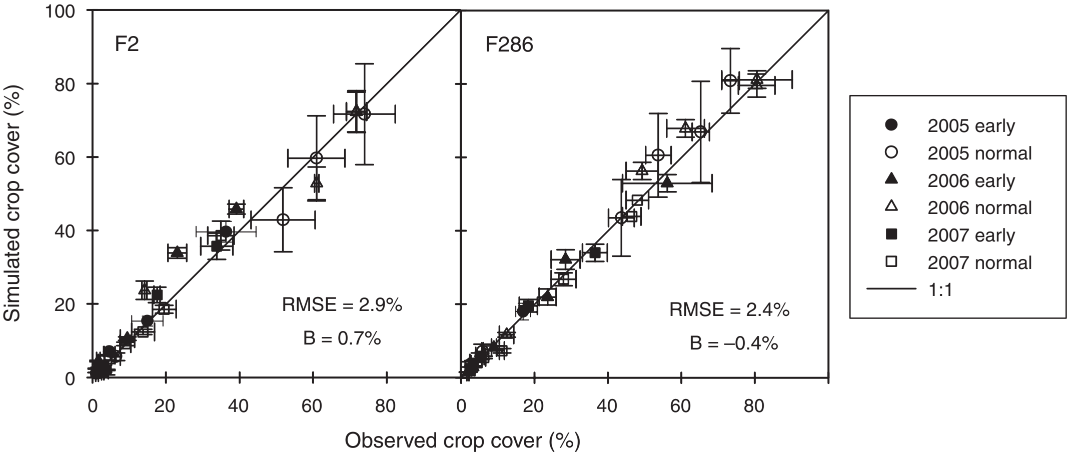

Fig. 3. Simulated *v.* measured ground cover for the maize lines F2 (left) and F286 (right). Data are for early and normal sowings in years 2005, 2006, and 2007. Bars indicate standard deviations ($n = 3$). RMSE, root mean square error; B, bias.

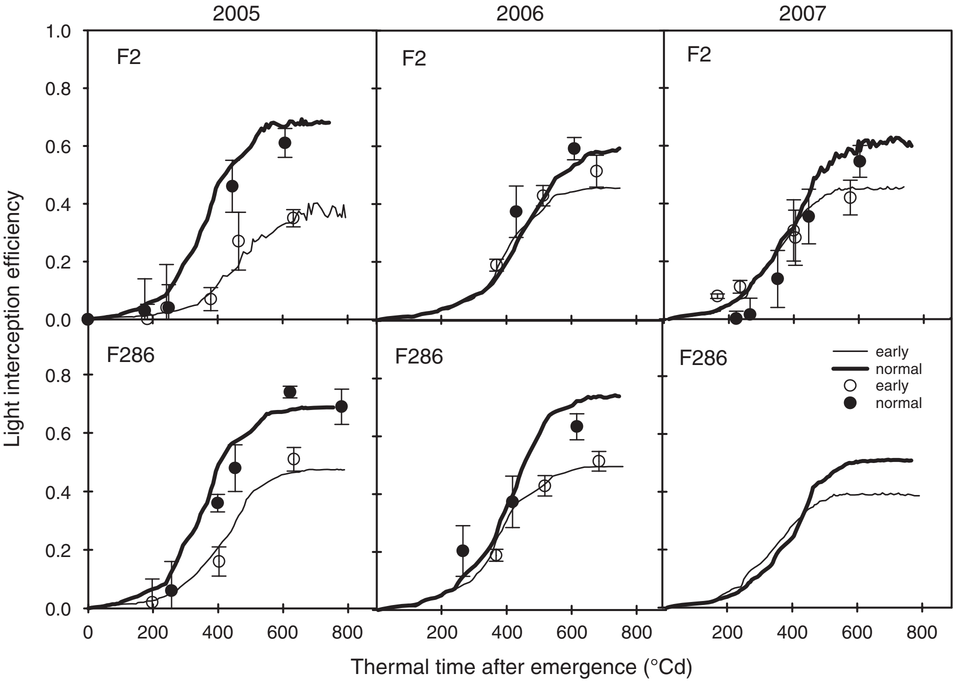

Fig. 4. Measured (dots) and simulated (lines) light interception efficiency, *v.* thermal time after emergence, for early and normal sowings of maize inbred lines F2 and F286 grown in 2005, 2006 and 2007. Bars show confidence intervals at $P = 0.05$. Owing to poor emergence rates, no direct measurements were available for F286 in 2007.

minimal in 2006. These results at flowering actually prolonged trends already existing at the end of seedling establishment (Fig. 5*a*). Further, even if slight differences in harvest periods changed maximal value rankings (plants were collected a few days later than stage seven liguled leaves in 2007 and display the highest values), reduction of productivity of early sowings at stage seven liguled leaves were significant and displayed an inter-annual pattern similar to that observed at flowering (2005 > 2007 > 2006).

The simulated intercepted PAR (PAR_c) is shown in Fig. 5*c*, *d*. As for dry matter productions, amounts of light captured varied significantly among treatments. We note that, patterns of variations of both PAR_c and biomass almost perfectly matched at flowering (Fig. 5*b*, *d*). PAR_c presented the same characteristic maximal values for both genotypes, as well as comparatively lower light interception for early sown treatments. In contrast, patterns of variations were clearly different earlier in the season (Fig. 5*a*, *c*). Values of PAR_c were even higher at the end of seedling establishment for early sowings of 2006 and 2007 than for their respective normal sowings. Such behaviour suggests that PAR_c plays a limited role in the biomass reductions during early growth stages, but that its role gets more prominent as the growing cycle progresses.

PAR_c values result from a combination of canopy's ability to capture light with a particular pattern of incoming PAR experienced during growth (Eqn 3). Crossing PAR_c values with light interception efficiencies (Fig. 4) enables us to specify whether climate or stand architecture is responsible for the observed variations (Fig. 5*b*, *d*). It appears from the ε_i kinetics that canopy architecture did not vary much among treatments during seedling establishment (thermal time <350°Cd), except in 2005 for the early sowing. Most of the variability between years or sowing dates in the PAR_c during this period resulted from differences in light availability (which was more favourable for early sowings in 2006 and 2007, resulting in higher PAR_c). Later in crop development, ε_i was systematically lower for early sown plants than for normal sowing kinetics so that both differences in stand architecture and in light availability contributed to PAR_c variability. Depending on the year the light climate either amplified (2005) or compensated (2006) for the differences resulting from the plant architectural traits of early and normal sowings (Fig. 5*d*).

Long-term radiation use efficiency (Fig. 5*e*, *f*.) was generally lower in early sowings than in normal sowings. The reduction was markedly more important during seedling establishment ($RUE_{early}/RUE_{normal} \sim 0.5$) than for the whole growth period ($RUE_{early}/RUE_{normal} \sim 0.9$). RUE also varied with the period, being higher between emergence and flowering than during seedling establishment. Conversely to PAR_c, this resulted in variations among treatments displaying more similarities with dry matter production during seedling establishment than later during the completion of the growth cycle. It suggests that RUE plays a prominent, but time-limited role in the biomass reductions of early sown plants.

Figure 6 shows the contributions of RUE and PAR_c to the variation in biomass between sowing dates as characterised by the k and $(1 - k)$ parameters (Eqn 6). It confirms that RUE did explain most of the reductions of productivity during early growth stages ($k > 0.65$, except for F2–2005 where $k = 0.45$), and PAR_c became the main contributor when the whole period from emergence to flowering was considered ($k < 0.5$). In 2006 and 2007, the light conditions were more favourable for the early sowing than for the late sowing. This resulted for the F2 genotype in a higher PAR_c in the early sowing than in the late sowing, partially compensating the negative impact of RUE on biomass production during early growth stages ($1 - k < 0$).

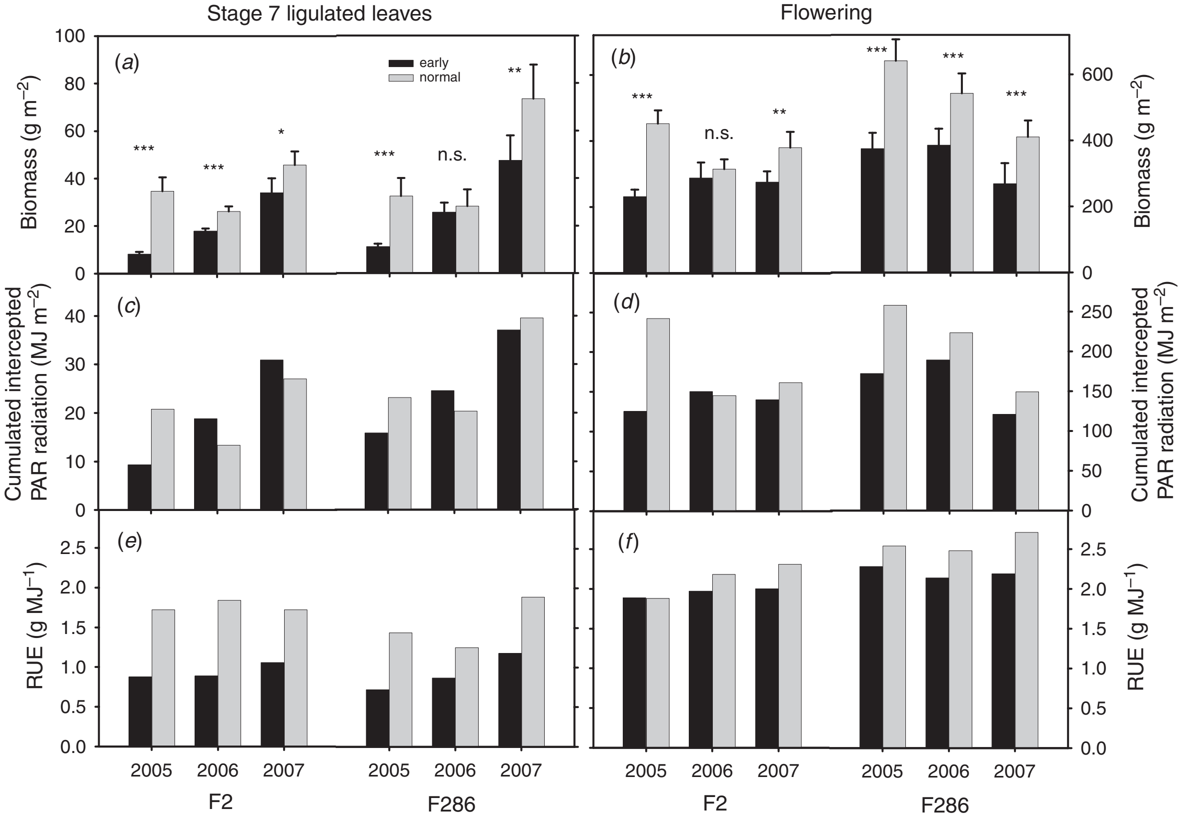

Fig. 5. (*a*, *b*) Biomass production, (PAR_c, *c*, *d*) cumulated intercepted PAR energy and (RUE, *e*, *f*) radiation use efficiency at stages seven liguled leaves and at flowering for early and normal sowing of maize inbred lines F2 and F286 grown in 2005, 2006, and 2007. Standard deviations and probability levels (*t*-test) are indicated for biomasses only, since PAR_c and RUE were derived from a single simulation of average plants in each case.

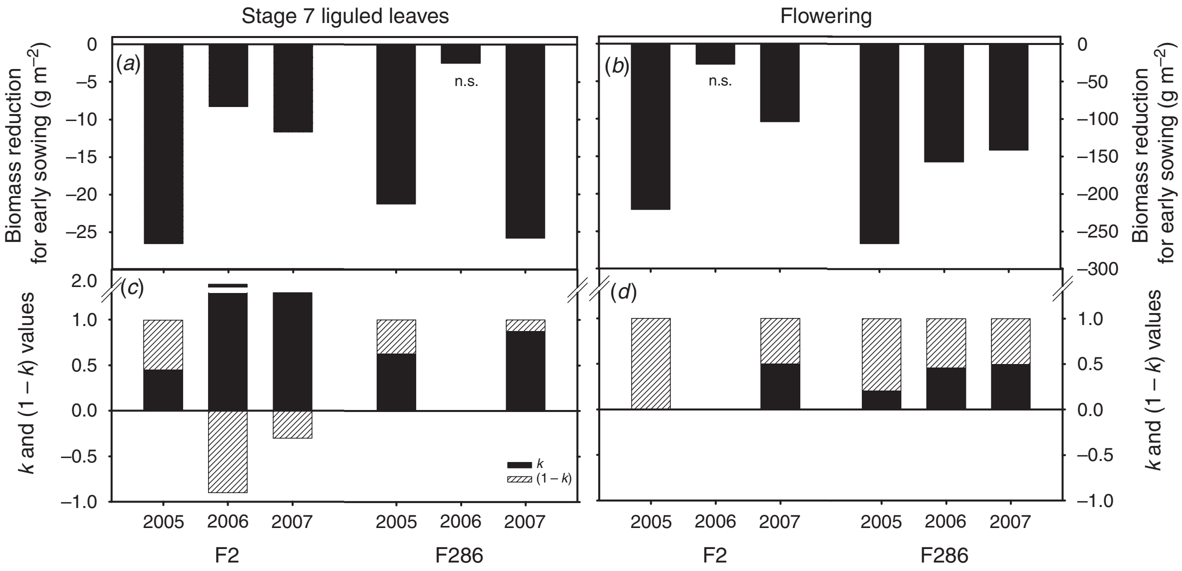

Fig. 6. (*a*, *b*) Difference between early and normal sowings in the biomass accumulated at stage seven liguled leaves and at flowering, and (*c*, *d*) contributions of radiation use efficiency (RUE) and of cumulated intercepted PAR (PAR_c), as represented by *k* and (1 – *k*) respectively, to the differences in biomass. Data are for maize inbred lines F2 and F286 grown in 2005, 2006 and 2007. Parameters *k* and (1 – *k*) (Eqn 6) were calculated only for cases where a significant difference in biomass existed between early and normal sowing.

Quantitative impact of cold on maize architecture and light interception

The relative contributions to ε_i of the main characteristics of maize architecture, namely plant developmental variables, organ dimensions and organ geometry (shape and orientation represented through average leaf elevations), were investigated. Table 3 presents the phyllochrons and leaf number results. Rates of leaf emergence (phyllochron^{-1}) differed between the two genotypes (ANCOVA, $P < 0.001$). F286 was quicker and its phyllochron remained unaffected by the sowing date for all the experiments. F2, however, displayed stable values for the 2006 and 2007 experiments only. In 2005, its phyllochron was significantly larger in the early sowing. Plant development was also modified in terms of final leaf number. A significant impact of both genotype (ANOVA, $P = 0.003$) and sowing date was observed on this variable, F2 and early sown plants had on average 0.5 and 0.8 fewer final leaves than F286 and normally sown plants, respectively. The number of senescent leaves at flowering remained unaffected, thus, the number of green leaves at this stage differed according to the difference in final leaf number.

Leaf dimensions and leaf elevations also differed among treatments (Fig. 7). The two lines displayed contrasting vertical profiles of leaf area (upper leaves being larger and

Table 3. Phyllochron, final leaf number and number of fully senesced leaves at flowering for early and normal sowings of maize inbred lines F2 and F286 of maize

Standard deviations are indicated into brackets. Phyllochrons were computed for the period from 50°Cd after emergence to 400°Cd after emergence (base temperature = 9.8°C). Probability levels (n.s., non-significant; *, $P < 0.05$; **, $P < 0.01$; ***, $P < 0.001$) refer to ANCOVA (phyllochron) and ANOVA (leaf numbers) results

Year		Phyllochron (°Cd)		Final leaf number		Fully senesced leaves at flowering	
		F2	F286	F2	F286	F2	F286
2005	early	62.6	48.1	11.8 (0.4)	13.0 (0.7)	5.6 (0.5)	5.8 (0.7)
	normal	49.1	47.7	12.6 (0.5)	13.3 (0.9)	5.1 (0.5)	6.2 (0.4)
2006	early	50.8	47.9	12.0 (0.5)	12.3 (0.9)	4.8 (0.4)	5.2 (0.5)
	normal	53.3	46.3	12.8 (0.7)	13.5 (0.9)	4.6 (0.5)	5.7 (0.5)
2007	early	45.4	41.3	12.2 (0.4)	12.6 (0.3)	4.6 (0.6)	4.9 (0.3)
	normal	46.5	43.9	13.2 (0.6)	13.3 (0.3)	4.9 (0.3)	4.7 (0.5)
Year (Y)		***	***	n.s.	n.s.	***	***
Sowing (S)		***	n.s.	***	***	n.s.	n.s.
Y × S		*	n.s.	n.s.	n.s.	n.s.	n.s.

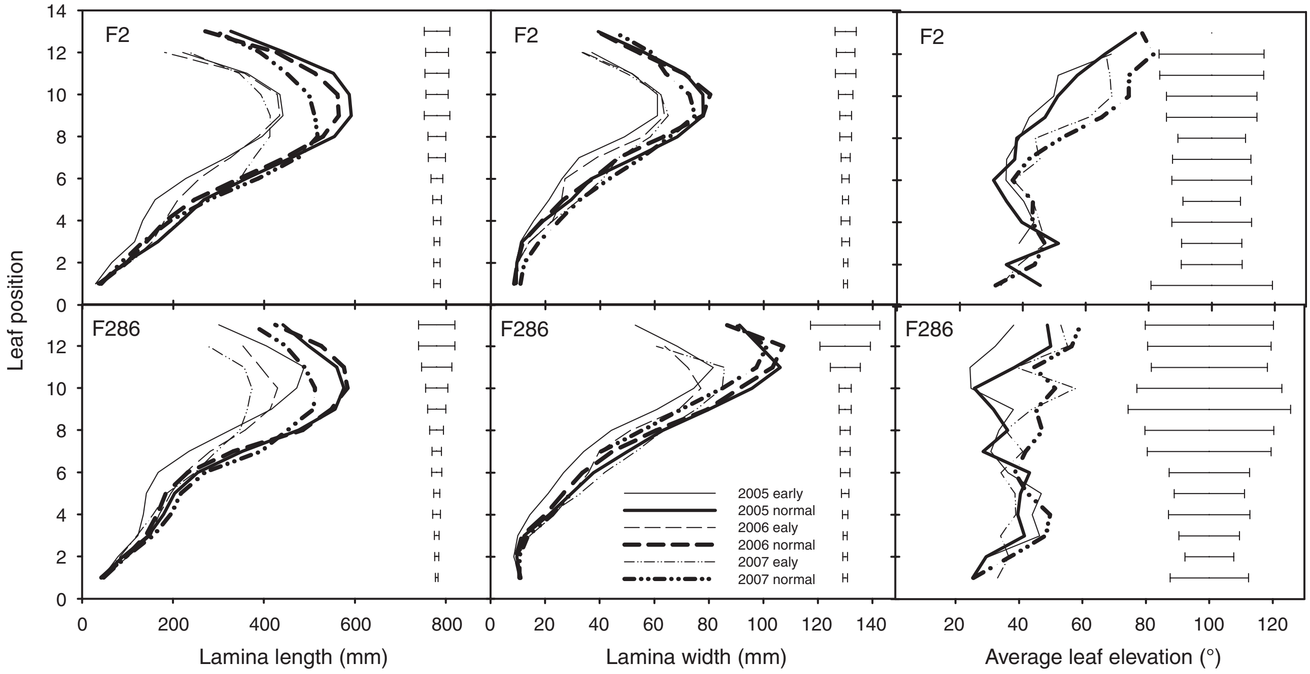

Fig. 7. Lamina length, lamina width and average leaf elevation for early and normal sowings of maize inbred lines F2 and F286 grown in 2005, 2006 and 2007. Horizontal bars show the confidence intervals at $P = 0.05$.

longer in F286) and of leaf elevations (more erect leaves in F2). Whatever the genotype, length and width of mature leaves were severely reduced for early sowings, the F2 line being more prone to this effect of suboptimal temperatures (in average there was a 45% reduction of plant leaf area for early sown F2, 35% for F286). In both lines, the differences between treatments in leaf area profiles followed a characteristic pattern. First, an envelope curve could be defined, corresponding to the leaf area profiles of normal sowing of 2005 and 2006. All other conditions resulted in leaf area profiles following the envelope for the lower leaves, and then dropping below the envelope for later leaves. The rank at which leaf area dropped below the envelope curve differed from year to year, but was identical for both lines. Leaf dimensions of early sowings were unaffected up to rank 3 in 2005, rank 4 in 2006 and rank 6 in 2007. The normal sowing of 2007 also displayed a significant departure from the envelope curve starting from rank 8. A correspondence could be established between these profile modifications and the climatic sequence experienced by the crop (Fig. 1). Departures from the envelope curve appeared related to the date of first occurrence of a significant thermal stress (early 2005 > early 2006 > early 2007 > late 2007 > late 2005 > late 2006), the first leaf rank with a significant reduction in size corresponding systematically to the leaf just following the one emerging at this date (Fig. 8).

In order to rank the different architectural traits with respect to their impact on PAR_c, we undertook a sensitivity analysis which

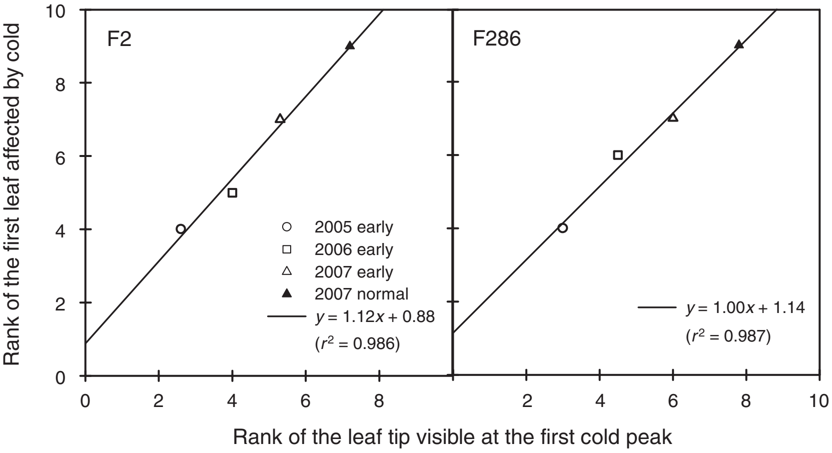

Fig. 8. Relationship between the rank of the first leaf displaying reduced dimensions and the rank of the leaf tip emerging at the peak of the first cold event.

involved contrasting scenarios of growth dynamics combining extreme situations of leaf dimensions, leaf angles and rates of leaf emergence (Table 4). It appeared that, at flowering, the most important variations in ε_i and PAR_c were explained by leaf dimensions (average increase of 56% in PAR_c when comparing paired scenarios only differing in their leaf profiles), whereas phyllochron (9%) and leaf angle (5%) contributed to a lesser extent. We note that whereas the phyllochron did contribute more than leaf angle at flowering, this would most likely be the opposite later in the cycle because of constitutively higher maximal light interceptions by the most planophile leaves. All other factors being equal, this indeed leads to differences of PAR_c that constantly increase after flowering in the first case, and that stop increasing at flowering in the second.

Quantitative impact of cold on RUE

Finally, the relationship between short-term RUE and the temperature conditions experienced by the crop was investigated (Fig. 9) to analyse the RUE variations observed at wider time scales (Fig. 5*e*, *f*). Short-term RUEs showed a large variability between dates, with however a clear trend to increase with plant development (Fig. 9*a*). Similar ontogenic-driven changes in RUE have already been reported on various crops (Hall *et al*. 1995; Campbell *et al*. 2001; Lecoeur and Ney 2003). So, we took the precaution of expressing this variable relative to a maximal value function of thermal time [RUE_{max}(TT)] to dissociate variations caused by ontogeny from potential disruptions generated by environmental factors. The RUE_{max} function was obtained by identifying a linear boundary line for the measured short-term RUEs plotted against thermal time. For each 100 degree day interval, the upper 10% of values were kept to establish the relationship. Air temperatures only explained a limited part of the time variation observed for these points ($r^2 < 0.3$ for the correlation between temperature and RUE_{max}, and $r^2 > 0.9$ between thermal time and RUE_{max}). The slopes of the boundary lines obtained were not significantly different between the two genotypes (ANCOVA, $P = 0.67$). Figure 9*b* presents the relationship between the resulting RUE/RUE_{max} ratio and air temperature. For the two lines, it followed a broken line pattern with similar thresholds of response to temperature (19.5 and 19.8°C for F2 and F286, respectively) and sensitivities to temperature reductions (ANCOVA, $P = 0.55$). The decline was particularly abrupt in the range 14–17°C.

Table 4. Sensitivity analysis results in terms of light interception efficiency (ε_i) and cumulated PAR energy intercepted (PAR_c) at flowering in maize

References to the corresponding growth scenarios (sen) of Table 2 are indicated in brackets

Leaf angle	Phyllochron	ε_i Leaf area profile		PAR_c (PAR MJ m^{-2}) Leaf area profile	
		–	+	–	+
–	–	0.43 (sen 1)	0.64 (sen 2)	131 (sen 1)	205 (sen 2)
–	+	0.43 (sen 3)	0.64 (sen 4)	142 (sen 3)	221 (sen 4)
+	–	0.46 (sen 5)	0.70 (sen 6)	138 (sen 5)	216 (sen 6)
+	+	0.46 (sen 7)	0.70 (sen 8)	152 (sen 7)	239 (sen 8)

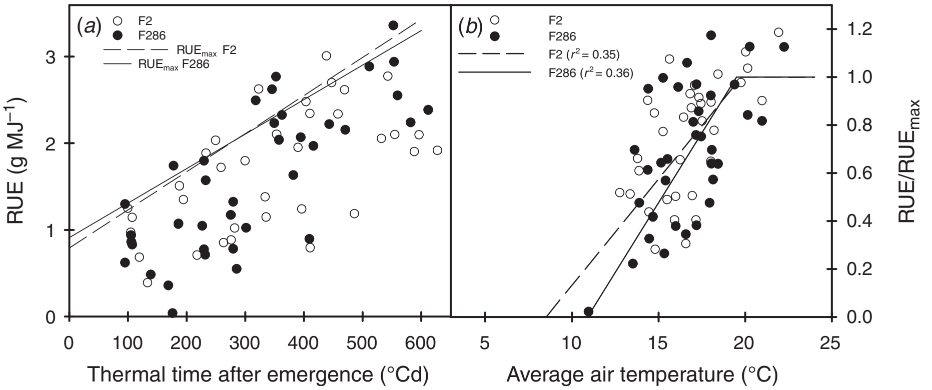

Fig. 9. (*a*) Radiation use efficiency (RUE) calculated between successive samplings, *v*. thermal time after emergence (TT), for early and normal sowings of maize inbred lines F2 and F286 grown in 2005, 2006, and 2007. Lines show the trend with thermal time of maximal radiation use efficiency (RUE_{max}) for F2 (dashed line) and F286 (full line). RUE_{max} fits were estimated from the upper 10% of values, for each 100 degree day interval. $RUE_{max} = 0.044TT + 0.79$ for F2 and $RUE_{max} = 0.041TT + 0.91$ for F286. Period of time between successive sampling is 7–12 days. (*b*) Relative radiation use efficiency (RUE/RUE_{max}) *v*. mean air temperature (T) for the conditions described above. Broken lines show the trend for F2 (dashed) and F286 (full line). In the temperature-sensitive part of the broken line, $RUE/RUE_{max} = 0.099T - 0.85$ for F2 and $RUE/RUE_{max} = 0.110T - 1.21$ for F286.

Discussion

Virtual plants as virtual sensors

Coupling an architectural model with a radiative model allow the estimation of light interception in highly heterogeneous environments (Chenu *et al.* 2005, 2008*b*; Rey *et al.* 2008). This modelling approach has been used here for early growth stages of maize, to overcome the limitations of direct measurement methods of light interception in highly heterogeneous canopies. Though mechanistic and partly forced with measurements, the combination of 3-D plant and light transfer simulation still implies numerous simplifying assumptions. Among these, simple and motionless 3-D representations, average organ dimensions and limited characterisation of the optical properties of plant elements are the most likely to affect light capture. They were globally evaluated using two canopy structure indices (ground cover, and ε_i) in view of their use in a quantitative tool.

Ground cover proved to be accurately simulated irrespective of considered crop growth stage, as shown by previous studies on narrower datasets (Fournier and Andrieu 1998; Evers *et al.* 2007). This suggests that the 3-D model was actually able to produce dynamic representations of maize stands conforming to the reality all along the growth cycle. Plant geometry is, however, evaluated according to a single direction of projection with this index (top-down pinhole projections of plant elements). Therefore, we further assessed simulation outputs on the basis of the targeted process to simulate: light interception. Once again, the model performed reasonably well. It satisfactorily reproduced the contrasted dynamics of ε_i observed among the combinations of sowing dates and genotypes. Occasional discrepancies with field measurements could be explained by the rather low power of spatial integration of sola, rimeters as compared with simulations (Gallo and Daughtry 1986; Sinclair and Muchow 1999) and potentially by over-simplified parameterisation of some model features (optical properties of the Déa cultivar, assumed unaffected by cold for instance). These results assess the feasibility and reliability of such a modelling approach to quantify light interception for maize seedlings as well as for mature plants of both genotypes. It is original in the sense that quantitative assessments of simulated 3-D plants are scarce and most focus on phylloclimate of mature plants and canopies (Fournier and Andrieu 1998; Casella and Sinoquet 2003; Louarn *et al.* 2008*a*).

The advantages of using architectural models are however not limited to their usefulness as virtual light sensors. As previously shown, they can also be used as a phenotyping tool to compare genotype behaviours in respect to their light interception (Chenu *et al.* 2007, 2008*b*; Rey *et al.* 2008) and give insight into the role of various architectural traits for resource capture (Pearcy and Yang 1996; Chenu *et al.* 2005; Louarn *et al.* 2008*b*). We performed a sensitivity analysis with these aims in mind (Table 4). The contribution of this original approach to solving practical questions addressed by breeders seeking to improve maize cold-tolerance is discussed in the next sections.

What limits maize productivity under cold temperatures?

When considering the effects of stresses on plant functioning, it is important to distinguish between stresses resulting in a reversible alteration of certain key processes and those resulting in a definitive impairment, due to inability to restore the function following removal of the constraint. Our results clearly demonstrated such a definitive impact of cold on final leaf dimensions and the ability of plants to capture light. Modifications of leaf area profile depended on the temperature sequence experienced, and more particularly on the time of first cold stress occurrence in the growth cycle. The first leaf rank with a significant reduction in size was always that of the next leaf to emerge at the time of first cold stress. This is consistent with the fact that no leaf area reduction were reported for normal sowings of 2005 despite of a cold event at nine liguled leaves (Fig. 1), because at this stage all the leaves are already visible. The reduction in size was then found for all upper leaves. These variations in leaf area profiles were the main reason for a lower $\mathrm{PAR_c}$ in early sowings (Table 4). As they last for the whole lifespan of the leaf, they induce cumulative effects on biomass production and the contribution of $\mathrm{PAR_c}$ increased all along the growing cycle. This is illustrated in 2005 when an early cold event highly reduced the growth of leaves 3 and upwards, which led to a reduction in biomass at flowering almost totally explained by the lower $\mathrm{PAR_c}$ (Fig. 6*c*). Grasses have to some extent the capacity to self-regulate the extension of new leaves according to the dimensions of previously grown leaves (Fournier *et al.* 2005; Andrieu *et al.* 2006). Thus, understanding whether a direct cold impact on very early stages of leaf extension, or the propagation of reduced size from lower leaves to upper leaves by self-adaptation, is responsible for the smaller size of late emerging leaves appears rather difficult. A direct impact on apex size or on very early growth of a trophic depletion engendered by low RUE during the critical heterotrophy-autotrophy transition cannot be set apart as shown recently on rice (Luquet *et al.* 2007).

By contrast, the lower efficiency in the conversion of intercepted light into biomass (RUE) played a prominent role during the period of cold stress (between seedling emergence and the stage seven liguled leaves in the range of climates tested), but tended to become marginal afterwards (Fig. 6*a*, *b*). An abrupt fall in short-term RUE was found when average weekly temperature was below 17°C (Fig. 9*b*). This threshold roughly corresponds to those reported to substantially decrease the carbon exchange rate at the leaf level (Greaves 1996; Janda *et al.* 1998; Massad *et al.* 2007). We note that contrary to the results by Richner *et al.* (1995), RUE variations were not explained here by cold-induced modifications in the allocation pattern to the root system, as for both genotypes the shoot : root ratio at the end of seedling establishment was unaffected by sowing date (shoot : root ratio measured in 2005 and 2006 at seven liguled leaves averaged 7.8 ± 0.9 and 8.1 ± 0.6 for early and normal sowings, respectively). The recovery of RUE after the stress may partly be explained by the leaf reversible response to chilling temperatures such as changes in chloroplast ultrastructure (Sowiński *et al.* 2005), decreases in quantum yield efficiency of the PSII (Smillie *et al.* 1988; Greer and Hardacre 1989; Aguilera *et al.* 1999) or impaired leaf gas exchange properties (Jones 1992). In addition, stresses occurred in the course of plant growth, when new functionally unaffected leaves continued to appear. As the last two leaves in expansion may represent as much as 50% of the total plant area (Ruget *et al.* 1996), the leaves having experienced a short stress during seedling establishment would represent a limited part of the plant surface in the following weeks.

In this context, identifying which process most likely limits dry matter production inevitably relates to the climate sequence the plants experienced. Indeed, if a single cold temperature event occurs shortly after emergence, cumulative effects of leaf area reduction on light interception will largely outdistance the effects of RUE that are transient and only affect the first few leaves, as observed in our study for the early sowings of 2005. Conversely, late chilling temperatures have a lower impact on light interception (as fewer leaves remain to expand) but alter temporarily the functioning of a wider leaf area (as more leaves have already expanded). Such a mechanism resulted in a major impact of RUE in the reduction of productivity observed in 2007 for early sown plants (Fig. 6*b*). Moreover, the effect of RUE reduction is likely to be strengthened in case of multiple cold events, or in autumn during the grain filling period when plant growth can no longer compensate for the RUE reduction (Ying *et al*. 2000).

Which consequences for maize selection?

Strategies for genetic improvement of maize involving altered low-temperature responses have so far mainly concentrated on how to avoid periods of stress, with selection of early-maturing photoperiod-insensitive hybrids (Derieux 1984). The method presented here to quantify the relative contributions of PAR_c and RUE to biomass production might be useful to characterise the varietal value of inbreds for cold-tolerance (as opposed to cold avoidance) in a given range of constraints. Proper selection of parent lines is indeed a critical step, particularly difficult to carry out when dealing with tolerant germplasm. The model-assisted phenotyping presented here proved capable of dissecting the genotype × environment (G × E) interaction for the two key traits driving productivity (i.e. RUE and PAR_c) in plants of two early maturing flint lines of European origin that were subjected to suboptimal temperatures. Such tool should also help in identifying relevant QTL to follow in genetic studies (Leipner *et al*. 2008; Letort *et al*. 2008) and could be used to prospect the genetic variability available for each trait (Greaves 1996). The present study, based on two lines only, was not designed to explore this. Nonetheless, some significant differences appeared, uncovering partially if not totally the genetic relevance of each trait.

Marked differences in plant architecture were shown between the two studied lines. F286 displayed more planophile leaves which were more efficient at intercepting incoming PAR all other factors being equal (Table 4). The vertical distribution of leaf area also differed, F286 having larger and longer upper leaves together with comparatively smaller basal leaves, irrespective of the treatment considered. These dissimilarities could result in noticeable modifications of ε_i at a given LAI (as shown on other crops, Rey *et al*. 2008), might modulate the response of the crop to a given climate and, as such, could be prospected as a potential margin of progress for cold adaptation. Similarly, a genetic variability was characterised for the sensitivities of leaf emergence rates (F286 always maintained its phyllochron in early sowing, while that of F2 was longer for the most severe stress) and leaf elongation rates (final leaf dimension were more affected in F2) to chilling temperatures (as shown previously by Miedema 1982; Giauffret *et al*. 1995; Lee *et al*. 2002), supporting the potential for improvement of leaf area establishment under cold temperatures.

The present results also enable us to challenge the potential variability in RUE. So far, breeding has probably not raised cereal RUE substantially under non-limiting environments (Reynolds *et al*. 2000). However, evidence for genetic variations has been demonstrated for the physiological phenomena supposed to account for the reduced rates of carbon assimilation under chilling temperatures (Dolstra *et al*. 1994; Sowiński *et al*. 2003; Fracheboud *et al*. 2004; Jompuk *et al*. 2005). Our results did not show any differences between the two studied lines in their maximal instantaneous RUE, in their threshold of response to temperature and in their sensitivities to temperature below this limit (Fig. 9). Far from closing the question, the methods developed here open new perspectives to quantitatively investigate the genotypic variability of this key trait during early growth stages.

Finally, this modelling approach could also be extended to analyse combination values and help define cold-tolerant hybrid ideotypes. This would require evaluation of how the relative contributions of each trait (PAR_c and RUE) are conserved in more vigorous plant materials. Indeed, the lines grown in the present study had maximal light interception (around 65%) and radiation use efficiencies (~$2.4\,g\,MJ^{-1}$) far below those usual for commercial hybrids (>90% and $3.5\,g\,MJ^{-1}$, respectively; Westgate *et al*. 1997; Lindquist *et al*. 2005). This might affect the relative importance of each trait. For instance, light interception is not linearly related to plant leaf area but saturates for Leaf Area Indices above $4\,m^2\,m^{-2}$, which are usually reached in commercial hybrids at flowering (Maddonni *et al*. 2001). The impact of leaf area reduction on ε_i could thus be weaker in commercial hybrids, and the contribution of PAR_c to variation in dry matter productivity of lesser importance. Experiments that aim to quantify this point are currently being conducted.

Acknowledgements

This study was supported by the Conseil Régional de Picardie (www.cr-picardie.fr) and INRA (www.inra.fr), France. We are grateful to M. Chelle for making the light transfer model available. We would also like to thank I Dourlen, J-F Hû and D. Rabier for their help with the experiment, and J. Hillier for the improvement of the manuscript.

References

Aguilera C, Stirling CM, Long SP (1999) Genotypic variation within *Zea mays* for susceptibility to and rate of recovery from chill-induced photoinhibition of photosynthesis. *Physiologia Plantarum* **106**, 429–436. doi: 10.1034/j.1399-3054.1999.106411.x

Andrieu B, Hillier J, Birch C (2006) Onset of sheath extension and duration of lamina extension are major determinants of the response of maize lamina length to plant density. *Annals of Botany* **98**, 1005–1016. doi: 10.1093/aob/mcl177

Ben Haj Salah H, Tardieu F (1995) Temperature affects expansion rate of maize leaves without change in spatial distribution of cell length. Analysis of the coordination between cell division and cell expansion. *Plant Physiology* **109**, 861–870.

Blondon F, Clabault G, Rainguez M (1980) Action d'une température fraîche (10°C) appliquée au stade jeune sur la croissance et l'activité photosynthétique de deux variétés précoces de Maïs. *Annales d'Amélioration des Plantes* **30**, 399–410.

Bonhomme R (2000) Beware of comparing RUE values calculated from PAR vs. solar radiation or absorbed vs. intercepted radiation. *Field Crops Research* **68**, 247–252. doi: 10.1016/S0378-4290(00)00120-9

Bonhomme R, Varlet-Grancher C (1978) Estimation of the gramineous crop geometry by plant profiles including leaf width variations. *Photosynthetica* **12**, 193–196.

Campbell CS, Heilman JL, McInnes KJ, Wilson LT, Medley JC, Wu G, Cobos DR (2001) Seasonal variation in radiation use efficiency of irrigated rice. *Agricultural and Forest Meteorology* **110**, 45–54. doi: 10.1016/S0168-1923(01)00277-5

Casella E, Sinoquet H (2003) A method for describing the canopy architecture of coppice poplar with allometric relationships. *Tree Physiology* **23**, 1153–1170.

Chelle C, Andrieu B (1998) The nested radiosity model for the distribution of light within plant canopies. *Ecological Modelling* **111**, 75–91. doi: 10.1016/S0304-3800(98)00100-8

Chenu K, Franck N, Dauzat J, Barczi JF, Rey H, Lecoeur J (2005) Integrated responses of rosette organogenesis, morphogenesis and architecture to reduced incident light in *Arabidopsis thaliana* results in higher efficiency of light interception. *Functional Plant Biology* **32**, 1123–1134. doi: 10.1071/FP05091

Chenu K, Franck N, Lecoeur J (2007) Simulations of virtual plants reveal a role for *SERRATE* in the response of leaf development to light in *Arabidopsis thaliana*. *New Phytologist* **175**, 472–481. doi: 10.1111/j.1469-8137.2007.02123.x

Chenu K, Chapman SC, Hammer GL, McLean G, Tardieu F (2008*a*) Short term responses of leaf growth rate to water deficit scale up to whole-plant and crop levels. An integrated modelling approach in maize. *Plant, Cell & Environment* **31**, 378–391. doi: 10.1111/j.1365-3040.2007.01772.x

Chenu K, Rey H, Dauzat J, Lydie G, Lecœur J (2008*b*) Estimation of light interception in research environments: a joint approach using directional light sensors and 3D virtual plants applied to sunflower (*Helianthus annuus*) and *Arabidopsis thaliana* in natural and artificial conditions. *Functional Plant Biology* **35**, 850–866.

Derieux C (1984) The main limiting factors of environment. In 'Physiologie du maïs'. (Ed. A. Gallais) pp. 383–387. (INRA: Paris)

Dolstra O, Haalstra SR, Van der Putten PEL, Schapendonk AHCM (1994) Genetic variation for resistance to low temperature photoinhibition of photosynthesis in maize. *Euphytica* **80**, 85–93. doi: 10.1007/BF00039302

Eagles HA, Hardacre AK (1979) Genetic variation in maize *(Zea mays* L.) for germination and emergence at 10°C. *Euphytica* **28**, 287–295. doi: 10.1007/BF00056585

Evers JB, Vos J, Fournier C, Andrieu B, Chelle M, Struik PC (2007) An architectural model of spring wheat: evaluation of the effects of population density and shading on model parameterization and performance. *Ecological Modelling* **200**, 308–320. doi: 10.1016/j.ecolmodel.2006.07.042

Fournier C, Andrieu B (1998) A 3-D architectural and process-based model of maize development. *Annals of Botany* **81**, 233–250. doi: 10.1006/anbo.1997.0549

Fournier C, Durand JL, Ljutovac S, Schäufele R, Gastal F, Andrieu B (2005) A functional–structural model of elongation of the grass leaf and its relationships with the phyllochron. *New Phytologist* **166**, 881–894. doi: 10.1111/j.1469-8137.2005.01371.x

Fracheboud Y, Jompuk C, Ribaut J, Stamp P, Leipner J (2004) Genetic analysis of cold-tolerance of photosynthesis in maize. *Plant Molecular Biology* **56**, 241–253. doi: 10.1007/s11103-004-3353-6

Fryer MJ, Oxborough K, Martin B, Ort DR, Baker NR (1995) Factors associated with depression of photosynthetic quantum efficiency in maize at low growth temperature. *Plant Physiology* **108**, 761–767.

Gallo KP, Daughtry CST (1986) Techniques for measuring intercepted and absorbed photosynthetically active radiation in corn canopies. *Agronomy Journal* **78**, 752–756.

Giauffret C, Bonhomme R, Derieux M (1995) Genotypic differences for temperature response of leaf appearance rate and leaf elongation rate in field-grown maize. *Agronomie* **15**, 123–137. doi: 10.1051/agro:19950204

Greaves JA (1996) Improving suboptimal temperature tolerance in maize – the search for variation. *Journal of Experimental Botany* **47**, 307–323. doi: 10.1093/jxb/47.3.307

Greer DH, Hardacre AK (1989) Photoinhibition of photosynthesis and its recovery in two maize hybrids varying in low temperature tolerance. *Australian Journal of Plant Physiology* **16**, 189–198.

Haldimann P (1998) Low growth temperature-induced changes to pigment composition and photosynthesis in *Zea mays* L. genotypes differing in chilling sensitivity. *Plant, Cell & Environment* **21**, 200–208. doi: 10.1046/j.1365-3040.1998.00260.x

Hall AJ, Connor DJ, Sadras VO (1995) Radiation use efficiency of sunflower crop: effects of specific leaf nitrogen and ontogeny. *Field Crops Research* **41**, 65–77. doi: 10.1016/0378-4290(94)00108-O

Heath MC, Hebblethwaite PD (1987) Seasonal radiation interception, dry matter production and yield determination for a semi-leafless pea (*Pisum sativum*) breeding selection under contrasting field conditions. *Annals of Applied Biology* **110**, 413–420. doi: 10.1111/j.1744-7348.1987.tb03273.x

Hutchinson BA, Matt DR, McMillen RT (1980) Effect of sky brightness distribution upon penetration of diffuse radiation through canopy gaps in a deciduous forest. *Agricultural and Forest Meteorology* **22**, 137–147.

Janda T, Szalai G, Ducruet JM, Páldi E (1998) Changes in photosynthesis in inbred maize lines with different degrees of chilling tolerance grown at optimum and suboptimum temperatures. *Photosynthetica* **35**, 205–212. doi: 10.1023/A:1006954605631

Jompuk C, Fracheboud Y, Stamp P, Leipner J (2005) Mapping of quantitative trait loci associated with chilling tolerance in maize (*Zea mays* L.) seedlings grown under field conditions. *Journal of Experimental Botany* **56**, 1153–1163. doi: 10.1093/jxb/eri108

Jones HG (1992) 'Plants and microclimate – a quantitative approach to environmental plant physiology.' (Cambridge University Press: Cambridge)

Lauer JG, Carter PR, Wood TM, Diezel G, Wiersma DW, Rand RE, Mlynarek MJ (1999) Corn hybrid response to planting date in the northern corn belt. *Agronomy Journal* **91**, 834–839.

Lecoeur J, Ney B (2003) Change with time in potential radiation use efficiency in field pea. *European Journal of Agronomy* **19**, 91–105. doi: 10.1016/S1161-0301(02)00019-9

Lee EA, Staebler MA, Tollenaar M (2002) Genetic variation in physiological discriminators for cold tolerance – early autotrophic phase of maize development. *Crop Science* **42**, 1919–1929.

Leipner J, Jompuk C, Camp KH, Stamp P, Fracheboud Y (2008) QTL studies reveal little relevance of chilling-related seedling traits for yield in maize. *Theoretical and Applied Genetics* **116**, 555–562. doi: 10.1007/s00122-007-0690-2

Letort V, Mahe P, Cournede P-H, De Reffye P, Courtois B (2008) Quantitative genetics and functional–structural plant growth models: simulation of quantitative trait loci detection for model parameters and application to potential yield optimization. *Annals of Botany* **101**, 1243–1254. doi: 10.1093/aob/mcm197

Lindquist JL, Arkebauer TJ, Walters DT, Cassman KG, Dobermann A (2005) Maize radiation use efficiency under optimal growth conditions. *Agronomy Journal* **97**, 72–78.

Long SP (1983) C_4 photosynthesis at low temperatures. *Plant, Cell & Environment* **6**, 345–363.

Long SP, East TM, Baker NR (1983) Chilling damage to photosynthesis in young *Zea mays*. I. Effects of light and temperature variation on photosynthetic CO_2 assimilation. *Journal of Experimental Botany* **34**, 177–188. doi: 10.1093/jxb/34.2.177

Louarn G, Lecoeur J, Lebon E (2008*a*) A three-dimensional statistical reconstruction model of grapevine (*Vitis vinifera*) simulating canopy structure variability within and between cultivar/training system pairs. *Annals of Botany* **101**, 1167–1184. doi: 10.1093/aob/mcm170

Louarn G, Dauzat J, Lecoeur J, Lebon E (2008*b*) Influence of trellis system and shoot positioning on light interception and distribution in two grapevine cultivars with different architectures – an original approach based on 3-D canopy modelling. *Australian Journal of Grape and Wine Research*, in press.

Luquet D, Song YH, Elbert S, This D, Clément-Vidal A, Périn C, Fabre D, Dingkuhn M (2007) Model-assisted physiological analysis of *Phyllo*, a rice architectural mutant. *Functional Plant Biology* **34**, 11–23. doi: 10.1071/FP06180

Maddonni GA, Otegui ME, Cirilo AG (2001) Plant population density, row spacing and hybrid effects on maize canopy architecture and light attenuation. *Field Crops Research* **71**, 183–193. doi: 10.1016/S0378-4290(01)00158-7

Massacci A, Iannelli MA, Pietrini F, Loreto F (1995) The effect of growth at low temperature on photosynthetic characteristics and mecanisms of photoprotection of maize leaves. *Journal of Experimental Botany* **34**, 177–188.

Massad RS, Tuzet A, Bethenod O (2007) The effect of temperature on C_4-type leaf photosynthesis parameters. *Plant, Cell & Environment* **30**, 1191–1204. doi: 10.1111/j.1365-3040.2007.01691.x

Meiri A, Silk WK, Lauchli A (1992) Growth and deposition of inorganic nutrient elements in developing leaves of *Zea mays* L. *Plant Physiology* **98**, 972–978.

Miedema P (1982) The effect of low temperature on *Zea mays*. *Advances in Agronomy* **35**, 93–128. doi: 10.1016/S0065-2113(08)60322-3

Monteith JL (1977) Climate and efficiency of crop production in Britain. *Philosophical Transactions of the Royal Society of London* **281**, 277–294. doi: 10.1098/rstb.1977.0140

Nie G-Y, Robertson EJ, Fryer MJ, Leech RM, Baker NR (1995) Response of the photosynthetic apparatus in maize leaves grown at low temperature on transfer to normal temperature. *Plant, Cell & Environment* **18**, 1–12. doi: 10.1111/j.1365-3040.1995.tb00538.x

Padilla JM, Otegui ME (2005) Co-ordination between leaf initiation and leaf appearance in field-grown maize (*Zea mays*): genotypic differences in response of rates to temperature. *Annals of Botany* **96**, 997–1007. doi: 10.1093/aob/mci251

Pearce RS (1999) Molecular analysis of acclimation to cold. *Plant Growth Regulation* **29**, 47–76. doi: 10.1023/A:1006291330661

Pearcy RW, Yang W (1996) A three-dimensional crown architecture model for assessment of light capture and carbon gain by understory plants. *Oecologia* **108**, 1–12. doi: 10.1007/BF00333208

Pollock CJ, Eagles CF (1988) Low temperature and the growth of plants. In 'Plants and temperature'. (Eds SP Long, FI Woodward) pp. 17–180. (Society for Experimental Biology: Cambridge)

Prévot L, Aries F, Monestiez P (1991) Modélisation de la structure géométrique du maïs. *Agronomie* **11**, 491–503. doi: 10.1051/agro:19910606

Prusinkiewicz P, Lindenmayer A (1990) 'The algorithmic beauty of plants.' (Springer-Verlag: New York)

Prusinkiewicz P, Hanan J, Hammel M, Měch R (1997) L-systems: from the theory to visual models of plants. In 'Plants to ecosystems: advances in computational life sciences'. (Ed. MT Michaelewicz) pp. 1–27. (CSIRO Publishing: Melbourne)

Rey H, Dauzat J, Chenu K, Barczi JF, Dosio JAA, Lecoeur J (2008) Using a 3-D virtual sunflower to simulate light capture at organ, plant and plot levels: contribution of organ interception, impact of heliotropism and analysis of genotypic differences. *Annals of Botany*, in press.

Reynolds MP, van Ginkel M, Ribaut J-M (2000) Avenues for genetic modification of radiation use efficiency in wheat. *Journal of Experimental Botany* **51**, 459–473. doi: 10.1093/jexbot/51.suppl_1.459

Richner W, Soldati A, Stamp P (1995) Shoot-root relations in field-grown maize seedlings. *Agronomy Journal* **88**, 51–61.

Rochette P, Desjardins RL, Pattey E, Lessard R (1996) Instantaneous measurements of radiation and water use efficiency of a maize crop. *Agronomy Journal* **88**, 627–635.

Ruget F, Bonhomme R, Chartier M (1996) Estimation simple de la surface foliaire de plantes de maïs en croissance. *Agronomie* **16**, 553–562. doi: 10.1051/agro:19960903

Rymen B, Fiorani F, Kartal F, Vanderpoele K, Inzé D, Beemster G (2007) Cold nights impair leaf growth and cell cycle progression in maize through transcriptional changes of cell cycle genes. *Plant Physiology* **143**, 1429–1438. doi: 10.1104/pp.106.093948

Sinclair TR, Horie T (1989) Leaf nitrogen, photosynthesis and crop radiation use efficiency: a review. *Crop Science* **29**, 90–98.

Sinclair TR, Muchow RC (1999) Radiation use efficiency. *Advances in Agronomy* **65**, 215–265. doi: 10.1016/S0065-2113(08)60914-1

Smillie RM, Hetherington SE, He J, Nott R (1988) Photoinhibition at chilling temperatures. *Australian Journal of Plant Physiology* **15**, 207–222.

Sowiński P, Rudzińska-Langwald A, Kobus P (2003) Changes in plasmodesmata frequency in vascular bundles of the leaf of *Zea mays* L. seedlings induced by growth at suboptimal temperatures in relation to photosynthesis and assimilate export. *Environmental and Experimental Botany* **50**, 183–196. doi: 10.1016/S0098-8472(03)00021-2

Sowiński P, Ridzińska-Langwald A, Adamczyk J, Kubica I, Fronk J (2005) Recovery of maize seedling growth, development and photosynthetic efficiency after initial growth at low temperature. *Journal of Plant Physiology* **162**, 67–80. doi: 10.1016/j.jplph.2004.03.006

Spitters CJT, Toussaint HAJM, Goudriaan J (1986) Separating the diffuse and direct component of global radiation and its implications for modeling canopy photosynthesis. 1. Components of incoming radiation. *Agricultural and Forest Meteorology* **38**, 217–229. doi: 10.1016/0168-1923(86)90060-2

Streit C (1992) 'Graphtal user manual.' (University of Bern: Switzerland)

Verheul MJ, van Hasselt PR, Stamp P (1995) Comparison of maize inbred lines differing in low temperature tolerance: effect of acclimation at suboptimal temperature on chloroplast functioning. *Annals of Botany* **76**, 7–14. doi: 10.1006/anbo.1995.1072

Verheul MJ, Picatto C, Stamp P (1996) Growth and development of maize (*Zea mays* L.) seedlings under chilling conditions in the field. *European Journal of Agronomy* **5**, 31–41. doi: 10.1016/S1161-0301(96)02007-2

Westgate ME, Forcella F, Reicosky DC, Somsen J (1997) Rapid canopy closure for maize production in the northern US corn belt: radiation-use efficiency and grain yield. *Field Crops Research* **49**, 249–258. doi: 10.1016/S0378-4290(96)01055-6

Yan W, Hunt LA (1999) An equation for modeling the temperature response of plants using only the cardinal temperatures. *Annals of Botany* **84**, 607–614. doi: 10.1006/anbo.1999.0955

Ying J, Lee EA, Tollenaar M (2000) Response of maize leaf photosynthesis to low temperature during the grain-filling period. *Field Crops Research* **68**, 87–96. doi: 10.1016/S0378-4290(00)00107-6

Manuscript received 8 March 2008, accepted 28 July 2008